COMPRESSIVE FAILURE OF NOTCHED GRAPHITE/EPOXY-HONEYCOMB SANDWICH PANELS

J. M. Mirazo M. G. Toribio and S. M. Spearing

Technology Laboratory for Advanced Composites
Department of Aeronautics and Astronautics, Massachusetts Institute of Technology,
Cambridge, Massachusetts 02139, U. S. A.

SUMMARY: Honeycomb sandwich panels with woven graphite-epoxy face sheets and Nomex^{TM} cores were manufactured with through-thickness slits as an experimental model for severe impact damage. The facesheets consisted of plain weave plies in $[0_3]$ and $[45/0_2]$ stacking sequences. Both material configurations showed a pronounced notch size effect. However, the two configurations were visually observed to exhibit different subcritical damage behaviors. In the $[0_3]$ material linear damage zones (consisting of fiber microbuckles or kink bands) propagated perpendicular to the loading direction, whereas in the $[45/0_2]$ material the visible subcritical damage consisted of bulging of the outer (45°) plies accompanied by interior delamination. Mechanics analyses of these two apparently distinct damage modes revealed that the linear damage zone is the dominant failure mode in ***both*** materials, and that the delamination buckling behavior is a secondary phenomenom.

KEYWORDS: honeycomb sandwich panel, damage tolerance, delamination, buckling, compression, linear damage zone.

INTRODUCTION

Honeycomb sandwich panels with composite facesheets offer a structurally efficient means of carrying bending loads. As such they have found extensive usage in aerospace applications for secondary structures and cabin applications such as floor beams and overhead compartments. However, there has been less use of honeycomb sandwich construction in primary load carrying structures, in part due to concerns over damage tolerance and the ability to repair such structures. Current design methodologies and the codes available for specifying repair procedures are still generally inadequate with regard to this issue. The approaches taken have typically focused on using experiments as the principal means of validating the design or repair. This results in a safe solution, but the high cost of fabricating large test structures and conducting the tests themselves adds to the expense of the process, and contributes further to the already unacceptably high cost of introducing composite materials. There is, therefore, a general need for an improved modeling capability for the damage tolerance of honeycomb sandwich structures. This is a particular example of a more widespread concern over the lack of an adequate predictive capability for composite structures [1].

A key parameter in assessing the damage tolerance of composite sandwich structures is the residual compressive strength. Damage (such as impact damage or interior delaminations) is often particularly deleterious to the compressive load carrying capability. Concern over this facet of damage tolerance has spawned semi-standard tests such as the post impact compression test [2] for non-honeycomb laminates. By comparison, relatively little work has focused on the damage tolerance of honeycomb sandwich structures [3,4].

This paper is focused on characterizing and developing models for the damage behavior of composite honeycomb sandwich panels containing open slits under uniaxial compression loading. These slits represent an experimental model for damage that might be encountered in service.

EXPERIMENTAL PROCEDURE

The honeycomb sandwich panels tested in this study consisted of 3-ply woven graphite epoxy facesheets (3k tows, plain weave) bonded to a 25.4 mm thick Nomex^{TM} (48 kg/m^3) core. Two facesheet stacking sequences were used, (0_3) and $(45/0_2)$, designated T0 and T45 respectively. Panels approximately 1m x 0.5 m were supplied by Boeing Commercial Airplane Group. The panels were machined into three sizes of test specimen, with round ended central slits that penetrated the full specimen thickness (i.e. facesheets and core). The ratio of slit size to specimen width was kept constant at 1/4. The diameters of the rounded ends of the slit were 6.4 mm in all cases. The specimen geometry is shown in figure 1 and the specimen dimensions are given in table 1.

	WxH (mm)	2a (mm)
Small	50.8 x 152.4	12.7
Medium	101.6x304.8	25.4
Large	203.2 x 406.8	50.8

Table 1. Specimen dimensions

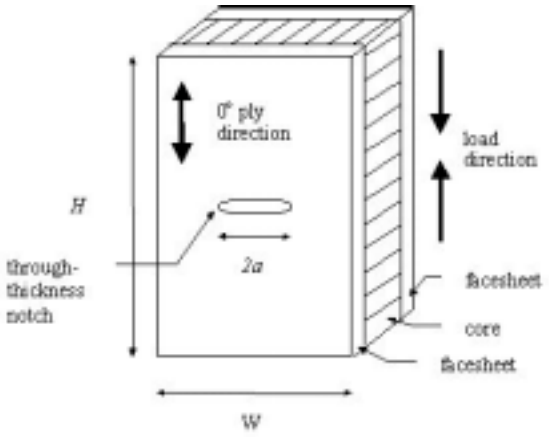

Figure 1. Test specimen schematic

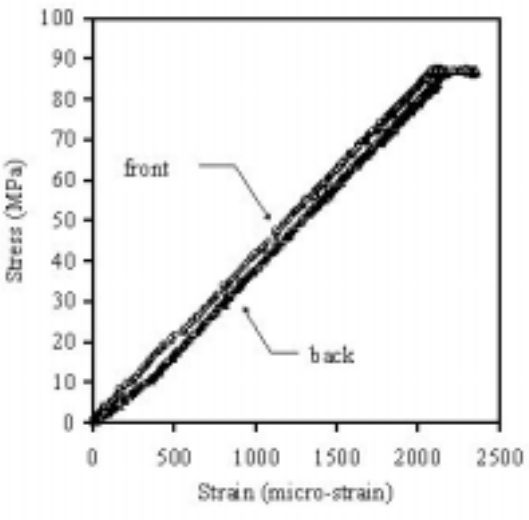

Figure 2. Typical stress-strain curve

Uniaxial compression loading was applied via a servohydraulic testing machine. The specimens were placed between a pair of flat compression platens, with the upper platen mounted on a damped ball joint so as to be self-aligning. Far field strain gauges on both faces of the specimens verified that bending strains were kept below 10% of the axial strain for all

tests, indicating an acceptable level of alignment. Once alignment had been verified, load was applied in displacement control at a rate of approximately 2 μm/s. Subcritical damage mechanisms were observed visually, and quantitative measurements of the lateral extent of the damage were made using a scale. In some cases tests were interrupted to allow the placement of strain gauges in the vicinity of the damage so as to monitor the residual load carrying capacity in the wake of the damage zone.

All coupons were loaded to failure. Since failure typically occurred in only one facesheet, it was possible to isolate the subcritical damage in the other facesheet for subsequent characterization. Damage characterization was performed *post mortem* for all specimens by sectioning the damaged regions, potting them in epoxy and progressively polishing to achieve a finish suitable for optical and scanning electron microscopy.

EXPERIMENTAL RESULTS/OBSERVATIONS

Mechanical Response

All specimens exhibited elastic behavior for the majority of the loading prior to ultimate failure. Some deviation from linear behavior was typically observed at loads greater than 90% of ultimate. A typical stress-strain plot is shown in figure 2.

The ultimate strength of the specimens showed a strong dependence on the specimen size with the larger specimens failing at lower stress, as shown in figure 3. In addition the $[45/0_2]$ material showed a lower strength than the $[0_3]$ material.

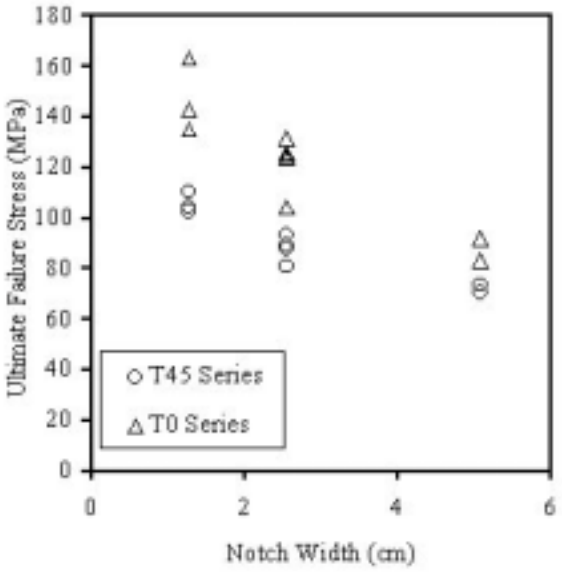

Figure 3. Hole size effect for specimens with (0_3) and $(45/0_2)$ facesheets

Damage Observations

In almost all cases some subcritical damage was observed on the specimen surfaces prior to final failure. This usually corresponded to the incidence of non-linearity in the load-displacement behavior. The two materials generally exhibited quite different damage behaviors, at least so far as could be observed on the surface. The $[0_3]$ material would show a "crack like" linear damage zone (LDZ) propagating from one or more of the notch tips perpendicular to the loading direction. The damage would be confined to a region less than 1 mm in axial extent. By contrast the $[45/0_2]$ specimens would usually show bulges in the outer plies, accompanied by a delamination between the 45° outer ply and the interior 0°

plies. Such delamination bulge zones (DBZ) were confined in their axial extent to the axial dimension of the notch (i.e. twice the notch root radius). Schematic representations of the macroscopic appearance of a LDZ and a DBZ are shown in figure 4. Corresponding micrographs are shown in figures 5 and 6.

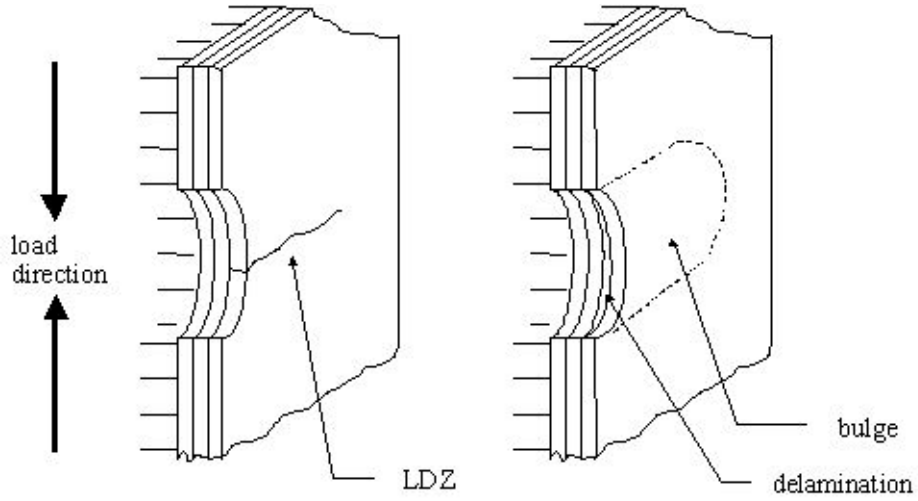

Figure 4. Schematic of linear damage zone and delamination buckle zone damage modes

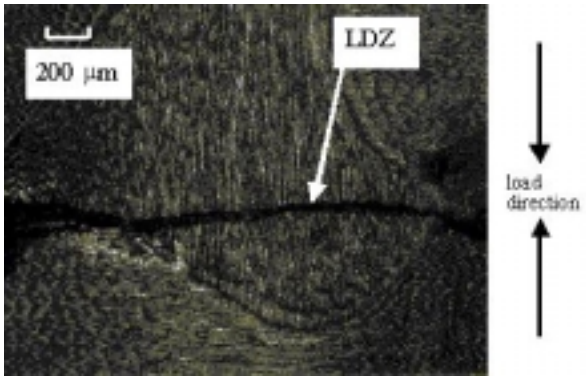

Figure 5. Micrograph of a linear Damage Zone (LDZ)

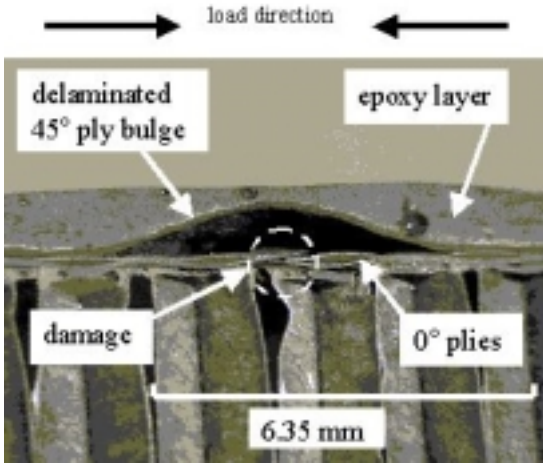

Figure 6. Micrograph showing a delamination/buckle zone (DBZ)

Closer inspection of the linear damage zone showed that the damage zone consisted of kink bands (figure 7) in the zero-degree tows of fibers, usually accompanied by delamination between the kinking ply and the other plies in the facesheet (figure 8).

Both forms of damage were observed to grow semi-stably, (i.e. in a series of short unstable propagation events) to lateral extents of about half the ligament width. Figure 9 shows a plot of LDZ length vs. applied load. In most cases the damage was observed to propagate at a nearly constant load, very close to the ultimate failure load. In several specimens axial strain gauges were attached slightly displaced from the predicted path of the damage. These permitted assessment of the strain distribution in the vicinity of the damage zone. Figure 10 shows data from one such experiment. There are two key observations, first, that as the damage zone approaches the line of a particular strain gauge the measured local strain

increases significantly, indicating a strain concentrating effect ahead of the damage zone. Then, once the damage tip has passed a given strain gauge the local strain decreases but does not drop to zero, indicating some residual load carrying capacity in the wake of the damage zone.

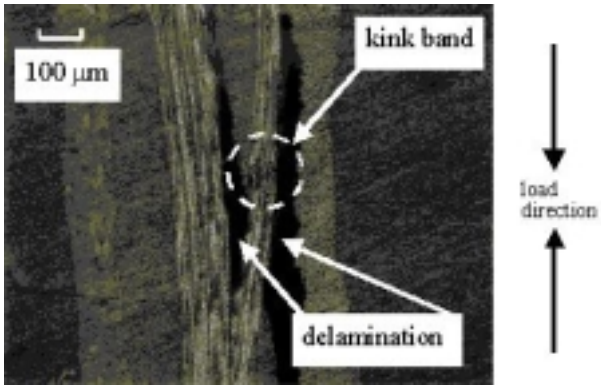

Figure 7. Micrograph showing a kink band accompanied by delamination

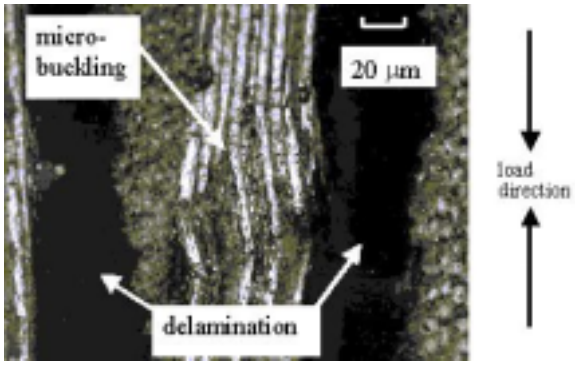

Figure 8 Micrograph showing a close up view of similar damage to that shown in figure 7.

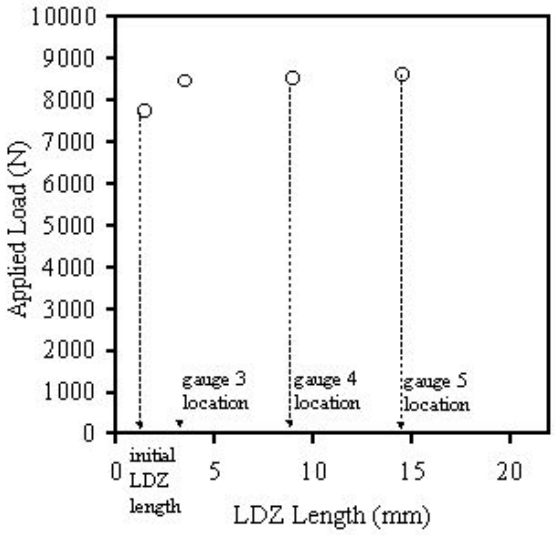

Figure 9. Damage zone length vs. applied load.

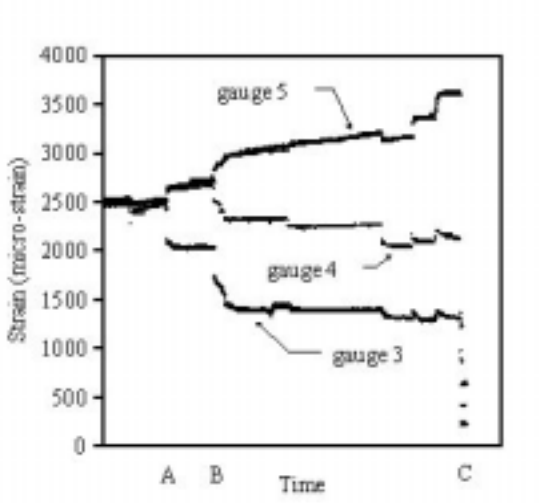

Figure 10. Local strain measurements as the damage zone grows past the gauge positions given in figure 9.

MODELING

In order to develop a predictive capability for the effects of damage on the load carrying capacity of the notched sandwich panels it is useful to construct models for the two principal damage modes observed in the experiments.

Modeling of the linear damage zone

The experimental observations of the linear damage zone suggest an analogy with a crack bridged by fibers growing in tension. This analogy has been explored previously by several workers for composite laminates loaded in compression [5-7]. The analytical treatment of the growth of such damage uses a fracture mechanics formalism where the crack tip stress intensity factor is determined by the applied stress intensity factor, and a shielding contribution due to the bridging tractions in the crack wake. The key to applying this modeling formalism is to identify the appropriate form for the bridging traction law used to model the load-displacement behavior of the kinking fibers in the wake of the linear damage zone. A linear strain-softening law was chosen for this purpose. An iterative solution method was used to solve the coupled problem of the crack tip stress intensity factor which depends on the damage modified crack opening displacement. From this the apparent resistance curve for the material can be predicted, assuming that the crack propagates at a constant value of the crack tip stress intensity factor. A complete description of the implementation of this model is available elsewhere [8,9]. Figure 11 shows the model fitted to the R-curves (expressed as an apparent toughness (in kJ/m^2)) obtained for the $[0_3]$ material. The stress and displacement parameters in the traction law, σ_c (the stress at zero crack closing displacement) and u_c (the crack closing displacement at zero stress) were 15 MPa and 350 μm respectively which are credible values based on the physical considerations such as the unnotched strength and the weave period.

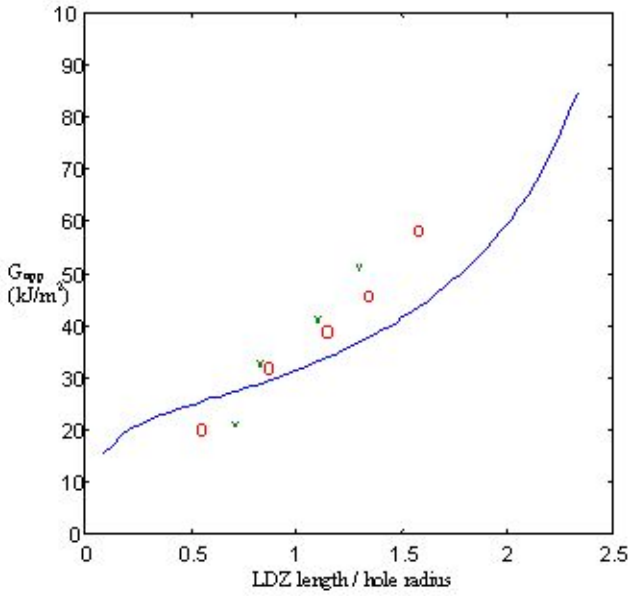

Figure 11. Linear damage zone resistance curve fitted to experimental data. The different specimen symbols refer to different specimens tested.

Modeling of the delamination buckle zone.

The propagation of a delamination/buckle zone perpendicular to the axis of loading with a constrained axial extent is a steady-state fracture problem, i.e. the conditions for crack advance do not depend on the crack length. This contrasts with similar delamination buckling problems in which the delamination/buckle grows parallel to the applied loading [10]. In order to solve this problem according to a fracture mechanics formalism it is only necessary to calculate the elastic strain energy stored in material far ahead of the damage zone tip and far in

its wake and the work done by the applied load going between the two. A schematic of the problem geometry is shown in figure 12. The advantage of this solution approach is that it avoids the need to consider the highly three dimensional problem associated with the curved delamination front at the bulge tip. It also provides a lower bound on the load required to propagate the delamination bulge. The energy stored and work associated with the strip of material ahead of the crack can be evaluated assuming that the material deforms axially according to Hooke's law. The energy and work associated with the strip of the material in the wake of the bulge can be evaluated assuming that the bulging plies behave as Euler columns with a characteristic load carrying capacity and an associated end shortening. The change in the total energy of the system associated with advance of the delamination bulge by a distance da, is the strain energy release rate available to propagate the delamination. The full derivation of the model is described elsewhere [8].

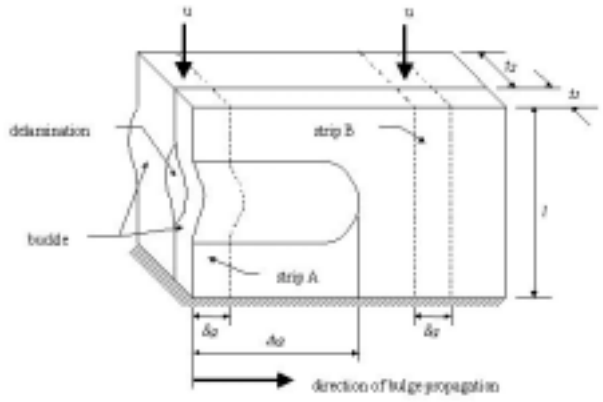

Figure 12. Schematic of DBZ.

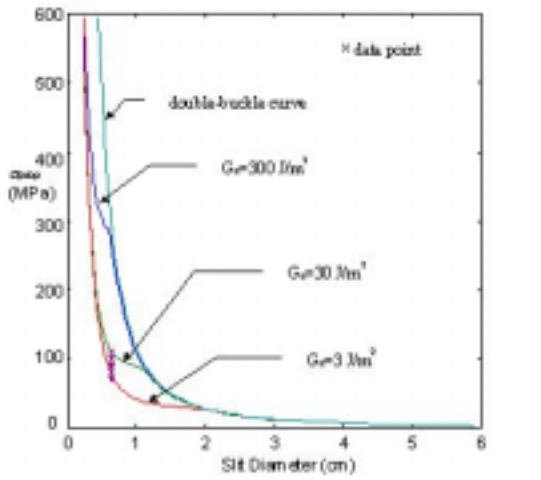

Figure 13. Predicted dependence of DBZ propagation stress on slit diameter as a function of delamination fracture resistance, G_c

Figure 13 shows the predicted applied stress for bulge propagation as a function of notch root diameter (which is assumed to constrain the axial extent of the damage), together with the experimental data. There is predicted to be no dependence on the notch size, although this is observed experimentally. In order to calibrate the model to the experimental data, given that the elastic constants and dimension of the specimens and material are well known, only the delamination toughness is relatively ill-defined. In order to fit the model to the data as shown in figure 14, a value of the delamination toughness of 3 J/m^2 was used. This is an unrealistically low value, compared to values in the range 150 J/m^2-600 J/m^2 typically measured using standard delamination test specimens.

DISCUSSION

Neither of the models briefly described here provide a complete description of the experimental observations. In particular it can be concluded that delamination/bulging is not a primary damage mode. The analytical results suggest that for a delamination/buckle to form, without other damage being involved, the delamination fracture resistance would have

to be exceptionally low. Closer examination of cross-sections, such as that shown in figure 6 indicated that DBZ's always appeared in conjunction with a kink band within the interior 0° plies. Furthermore, calculation of the 0° ply stress at ultimate failure of the $(45/0_2)$ specimens shows that it is almost identical to that measured in the (0_3) specimens. Figure 15 shows the data of figure 3 replotted with a comparison of the nominal 0° ply stress. The coincidence of the data suggests strongly that only the failure of the 0° plies is important in determining the ultimate strength of these materials. Furthermore, it seems as though the surface appearance of the delamination bulge is merely tracking a LDZ propagating in the subsurface 0° plies. Presumably the higher strain to failure of the 45° plies, combined with their lower stiffness, makes it energetically favorable for them to delaminate and buckle rather than to allow a damage zone to form on the same line as the kink band in the interior plies. It can therefore be suggested that a complete model for kink-band formation would be appropriate for describing the failure or damage tolerance of materials in which 0° fibers dominate the load carrying capacity.

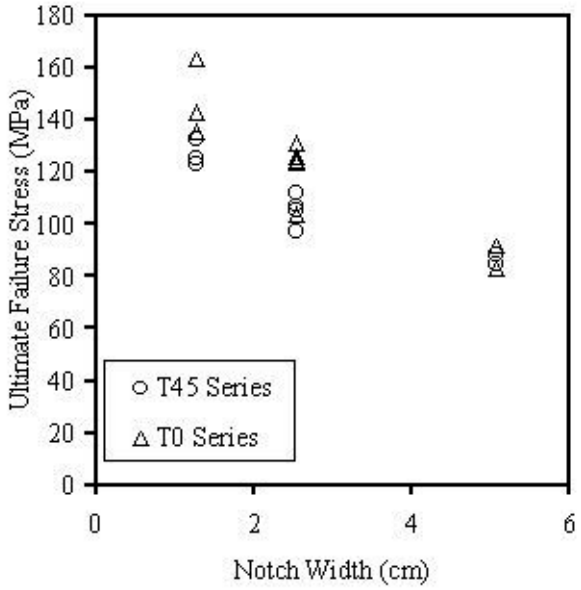

Figure 14. Data from figure 3 recalculated in terms of the 0° ply failure stress.

CONCLUSIONS

Experimental results and damage observations have been presented for honeycomb sandwich panels containing through-thickness slits. A significant specimen size effect was observed in both materials containing $[0_3]$ woven graphite fiber/epoxy facesheets and those with a $[45/0_2]$ stacking sequence of the same facesheet material. The two material types apparently exhibited macroscopically different damage behavior, with linear damage zones forming in the $[0_3]$ material and delamination/bulge zones in the $[45/0_2]$ material. However, closer inspection suggested that the delamination/bulge behavior was a secondary manifestation of the formation of a linear damage zone in the interior 0° plies. A fracture mechanics analogue of a fiber-bridged crack loaded in tension allows the LDZ growth to be modeled using a linear strain-softening law for the load carrying capacity of the material in the wake of the LDZ tip. Future work is required to more accurately describe the initiation of such damage and to link the initiation and growth of such damage to the ultimate strength and thence to predictions of damage tolerance.

ACKNOWLEDGEMENTS

The work described herein was supported by a contract from Boeing Commercial Airplane Group (# X-25685) and a CAREER award (#CMS-9702399) from the National Science Foundation. Technical discussions with Dr. Hamid Razi are gratefully acknowledged.

REFERENCES

1. Lagace, P. A., Spearing, S. M., and. McManus, H. L. N., "A Proposed Design Methodology for the Failure and Durability of Composite Structures," presented at 11th DoD/NASA/FAA Conference on Fibrous Composites in Structural Design, Fort Worth, TX, Aug 1996.
2. Lee, S. M., "Compression-After-Impact of Composites with Toughened Matrices", *SAMPE Journal*, **22**: (2) 64-68, 1986.
3. Scarponi C, Briotti G, Barboni R, Marcone A, Iannone M "Impact testing on composites laminates and sandwich panels", J. Composite Materials, **30**, 1873-1911 1996.
4. Kassapoglou, C, Jonas, P.J. and Abbott, R. "Compressive Strength of Composite Sandwich Panels after Impact Damage – An Experimental and Analytical Study," *J. Composites Technology and Research* **10** 65-73 1988.
5. Budiansky, B. and Fleck, N. A., "Compressive Failure of Fibre Composites", *J. Mech. Phys. Solids*, **41** 183-211, 1993.
6. Guynn, E. G., Bradley, W. L and Elber, W. "Micromechanics of Compression Failures in Open Hole Composite Laminates", Composite Materials: Fatigue and Fracture, Second Volume, ASTM STP 1012, Paul A. Lagace Ed., American Society for Testing and Materials, Philadelphia, pp. 118-136, 1989.
7. Soutis, C., Fleck, N. A., and Smith, P. A., "Failure Prediction Technique for Compression Loaded Carbon Fibre-Epoxy Laminates with Open Holes", *Journal of Composite Materials*, **25** pp 1476-1498, 1991.
8. Mirazo, J. M., "Damage Characterization and Modeling of Notched Graphite/Epoxy Sandwich Panels in Compression", S. M. Thesis, MIT 1999.
9. Toribio, M. G., "Damage Characterization and Modeling of Notched Glass/Epoxy Sandwich Panels in Compression", S. M. Thesis, MIT 1999.
10. Cox, B.N. "Delamination and Buckling in 3D Composites", *J. Composite Materials*, **28** 1114-1126 1994.